

Water-Soluble Pentagonal-Prismatic Titanium-Oxo Clusters

Guanyun Zhang,[†] Caiyun Liu,[†] De-Liang Long,[‡] Leroy Cronin,[‡] Chen-Ho Tung,[†] and Yifeng Wang^{*,†}

[†]Key Lab for Colloid and Interface Science of Ministry of Education, School of Chemistry and Chemical Engineering, Shandong University, Ji'Nan 250100, P. R. China

[‡]WestChem, School of Chemistry, University of Glasgow, Glasgow G12 8QQ, United Kingdom

S Supporting Information

ABSTRACT: By using solubility control to crystallize the prenucleation clusters of hydrosol, a family of titanium-oxo clusters possessing the $\{Ti_{18}O_{27}\}$ core in which the 18 Ti(IV)-ions are uniquely connected with μ -oxo ligands into a triple-decked pentagonal prism was obtained. The cluster cores are wrapped by external sulfate and aqua ligands, showing good solubilities and stabilities in a variety of solvents including acetonitrile and water and allowing their solution chemistry being studied by means of electrospray ionization mass spectroscopy, ^{17}O NMR, and vibrational spectroscopy. Furthermore, this study provides new titanium oxide candidates for surface modifications and homogeneous photocatalysis.

Metal oxide clusters constitute a large and rapidly growing class of discrete molecular materials that are useful in a variety of applications such as homogeneous catalysis, solution chemistry studies, and surface functionalization.¹ Among them, titanium-oxo clusters² are especially attractive for their roles as prenucleation clusters and as molecular analogues of titanium oxides³ such as TiO_2 , which has been the most important photocatalyst to date.⁴ Over the past six decades,⁵ most titanium-oxo clusters were produced as isolated intermediates from nonaqueous solvothermal synthesis of TiO_2 nanomaterials.^{3b,c,6} These compounds are passivated with alkoxide ligands or chelating carboxylate ligands and are sensitive to H_2O and oxidative environments, which largely limit their potential applications like solar light harvesting.^{3b,c,6} However, titanium-oxo clusters isolated from water without any additional (chelating) ligands, which can be regarded as the prenucleation clusters⁷ of titanate hydrosol, are very rare,⁸ while those among them that can be redissolved as stable and individual ions in solvents like water have not been reported.

$TiOSO_4$ and $TiCl_4$ are the most common precursors for the aqueous sol-gel synthesis of titanate nanomaterials. We recently demonstrated that even when they are dissolved as clear aqueous solutions under highly acidic conditions Ti(IV) spontaneously hydrolyze and condensate into titanium-oxo oligomers.^{8a,b} With the coexisting ions to lower the solubilities, some low-nuclearity prenucleation titanium-oxo clusters could be selectively isolated.

Herein, we have moved a big step forward and report a new type of 18-nuclear titanium-oxo clusters (e.g., $[Ti_{18}O_{27}(OH_2)_{30}(SO_4)_6]^{6+}$, **1a**, in Figure 1) passivated with SO_4^{2-} and aqua ligands. The 18 titanium atoms are connected with μ_2 -O and μ_3 -O into a unique pentagonal triple-decked cylindrical metal-oxide geometry. Compound **1a** $Cl_6 \cdot 6TBAC$.

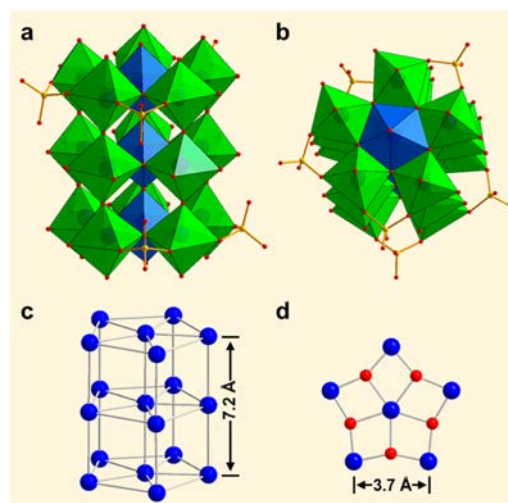


Figure 1. (a) Side and (b) top views, (c) the triple-decked arrangement of the 18 Ti atoms, and (d) the $\{Ti(Ti_5)\}$ pentagonal building unit, in the structure of $[Ti_{18}O_{27}(OH_2)_{30}(SO_4)_6]^{6+}$ (**1a**). Color scheme: Ti, blue; O, red; S, yellow. For clarity, hydrogen atoms at the aqua ligands are omitted. In panels a and b, Ti atoms are at the centers of the green octahedra and the blue pentagonal bipyramids, and oxygen atoms lie at the vertices of the polyhedra.

$12H_2O$ (**1**; TBAC = tetrabutylammonium chloride) exhibiting a $Ti_{18}O_{27}$ core structure was isolated by precipitation of prenucleation species of TiO_2 from the Ti^{4+}/SO_4^{2-} system by using TBAC. Electrospray ionization mass spectrometry (ESI-MS), ^{17}O NMR, and solution vibrational spectra were used to study their solution chemistry upon redissolution in a variety of solvents including water. They were further applied in surface functionalization of graphene oxide (GO) and tested as active molecular titanium oxide photocatalysts.

The titanium oxide core in **1a** can be viewed as a decked trimer (Figure 1c) of three near-planar pentagonal $\{Ti(Ti_5)\}$ building units (Figure 1d) connected with μ_2 -O atoms with a layer-to-layer distance of ca. 3.6 Å. In the center of each pentagonal $\{Ti(Ti_5)\}$ building unit locates a seven-coordinated Ti^{IV} -center, which is connected through five μ_3 -O atoms with five six-coordinated Ti^{IV} -centers distributed nearly evenly at the vertices. All the Ti-atoms are in their highest oxidation state, i.e., +4, as indicated by the colorless appearance and the electron spin resonance of **1**. Bond valence sum (BVS) calculations indicate

Received: June 17, 2016

Published: August 15, 2016

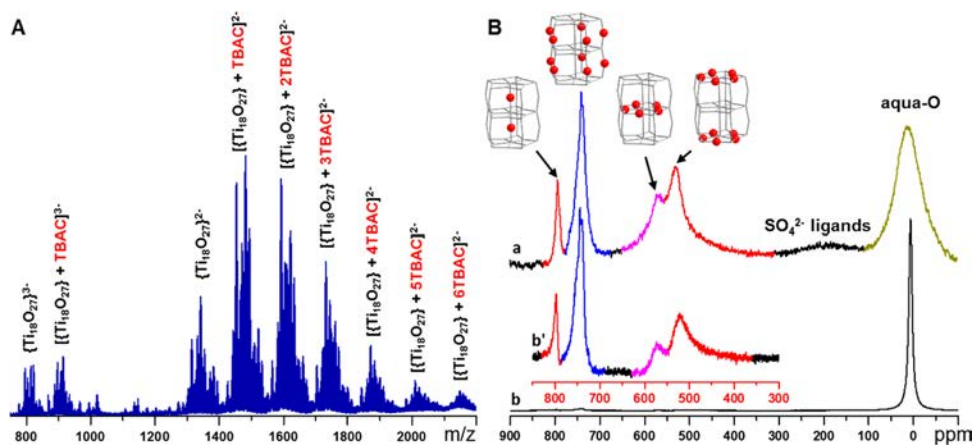


Figure 2. (A) Negative mode ESI–MS of **1** in MeCN and (B) ^{17}O NMR spectra of the ^{17}O -enriched **1** in MeCN (a) and in ^{17}O -enriched water (full spectrum b and the magnified view b'). Detailed MS peak assignments are included in Table S2.

that none of the bridging O atoms is protonated, and meanwhile, the 30 terminal-O are actually aqua ligands, related to the very low acidity of an aqua ligand bonded to the cluster surface (Table S1). Cluster **1a** is also capped with six bridging bidentate SO_4^{2-} ligands on the longitude surface of the $\text{Ti}_{18}\text{O}_{27}$ core. Due to the locations of the SO_4^{2-} ligands, **1a** internally possesses planar chirality (Figure S1). Both enantiomers are present in the unit cell, leading **1** to a racemic material.

In the coordination chemistry of transition metals, the $\{\text{M}(\text{M}_5)\}$ (M = metal) pentagonal unit is a very important transferable building block⁹ in the formation of metal-oxide clusters. They are normally seen in molybdates and are rare for other iso-polyoxometalates.^{1b,9,10} Although recently the $\{\text{M}(\text{M}_5)\}$ units are also seen in W-,^{10a,11} Nb-,¹² and Ti-¹³ oxo complexes, they prevalently form the highly curved outer surfaces of spheroidal clusters like the Keplerate $\{\text{Mo}_{132}\}$ ^{10c} and the fullerene-like $\{\text{Ti}_{42}\}$ oxoalkoxide^{13a} by appropriate linkers or sharing edges. Herein the triple-decked geometry of the pentagonal building blocks in **1a** demonstrates their potential for construction of nonspheroidal molecular structures.

Compound **1** could be readily dissolved in common polar solvents like acetonitrile (MeCN, 300 mM), water (150 mM in 1.0 M HCl), methanol (180 mM), ethanol (140 mM), isopropanol (80 mM), acetone (140 mM), tetrahydrofuran (80 mM), nitromethane (100 mM), and benzyl alcohol (50 mM). ESI-MS was then used to investigate the stability of **1a** in MeCN. Association/dissociation of H_2O , SO_4^{2-} , Cl^- , TBA^+ , and H^+ can occur during desolvation (180 °C by ESI) of the polycationic $\{\text{Ti}_{18}\text{O}_{27}\}$ clusters, resulting in both positively and negatively charged species. In the ESI⁻ mode (Figure 2A), the two ensembles of related clusters in the range from 750 to 950 are attributed to the species $\{\text{Ti}_{18}\text{O}_{27}\}^{3-}$ and $[\{\text{Ti}_{18}\text{O}_{27}\} + \text{TBAC}]^{3-}$, respectively. The species in the range of 1260 to 2250 are all -2 charged species with continuously increasing numbers of TBAC molecules (Table S2). Observation of the ensembles of the related clusters with differing numbers of TBAC, which follow both the -2 and the -3 species, strongly supports the assignments. The ESI-MS in the positive mode was also performed, and the data agree well with the structural stability of **1a** (Figure S3).

To gain further insight into the solution chemistry of **1a**, ^{17}O NMR spectroscopy on ^{17}O -labeled **1** was carried out.¹⁴ ^{17}O -labeled **1** was conveniently prepared following the same protocol as normal **1** but using 10% ^{17}O enriched water. The ^{17}O NMR

spectrum of **1** in MeCN (Figure 2B, curve a) shows five resonances related to the O-ligands. The relatively broad peak at 0 ppm is assigned to the quickly exchanging aqua ligands and solvent water. The peak at 528 ppm is assigned to the 10 μ_3 -O in the top and the bottom $\{\text{Ti}(\text{Ti}_5)\}$, while that at 569 ppm is assigned to the five μ_3 -O in the middle $\{\text{Ti}(\text{Ti}_5)\}$ (see the cartoons in Figure 2B).¹⁴ The two peaks at 738 and 793 ppm are assigned to the 10 μ_2 -O near the surface and the two buried in the $\text{Ti}_{18}\text{O}_{27}$ framework, respectively. Their relative intensity, defined as ratio of the peak area, is close to the expected 42:10:5:10:2 (from the high field to the low field; both the O-ligands and the solvent water in **1** are accounted). The well-resolved peaks and the match of the experimental peak area ratio to the solid-state structure suggest that exchange of the oxo-ligands with the aqua-O atoms is slow comparing to the time scale of the ^{17}O NMR measurements. A downfield-shifted resonance of the bridging-O atoms buried in the $\text{Ti}_{18}\text{O}_{27}$ framework relative to those near the surface is observed (e.g., 569 vs 528 ppm of the μ_3 -O), which can be attributed to a weaker shielding effect of the titanium-oxo framework to the buried O atoms, originating from the stronger bonding with Ti. Broadening of the signals is attributed to the magnetic nonequivalence and/or the high nuclear quadrupole relaxation of the O atoms.¹⁵ The ^{17}O NMR spectrum of a fully hydrated, free SO_4^{2-} ion has a sharp signal at 162 ppm (Figure S4), but this was not seen in the ^{17}O NMR of **1**, and instead, a very broad signal near this region is observed, suggesting SO_4^{2-} ligands are not dissociated from the $\text{Ti}_{18}\text{O}_{27}$ framework.

The ^{17}O NMR of **1** in ^{17}O -enriched 1.0 M HCl solution shows five resonance peaks whose locations are consistent with the peaks of **1a** in MeCN (Figure 2B). Due to the high concentration of ^{17}O in the solvent, phase correction cannot be precisely performed. The relative peak intensity of the μ_2 -O on the surface and those buried in the $\text{Ti}_{18}\text{O}_{27}$ framework is near to 5:1, and meanwhile, the relative peak intensity of the μ_3 -O on the surface and those buried in the titanium-oxo framework is nearly 2:1, both indicating the integrity of the $\text{Ti}_{18}\text{O}_{27}$ framework in acidic water.

The Fourier transform infrared spectroscopy (FTIR) of **1** in MeCN solvent is well-consistent with that of the authentic solid sample. The frequencies at 839 and 738 cm^{-1} assigned to Ti-(O_μ) and Ti-(OH_2) of **1** (Figure S5),^{8a,b} respectively, are slightly shifted to higher frequencies upon dissolution in MeCN, and meanwhile, the absorbance and the concentration follow the Beer–Lambert law (Figure S6). Air-drying of the solution gives a

solid whose IR indicates it is **1**. In the Raman spectra, the frequencies of the SO_4^{2-} ligands in the ranges of 400–600 and 930–1030 cm^{-1} and those of Ti–O in the range of 100–250 cm^{-1} are maintained in MeCN solution. Further, the solution vibrational spectra remained unchanged upon aging for a few months under ambient conditions, indicating the stability of **1** in MeCN with time. The above solution stability results are consistent with the ESI-MS and the ^{17}O NMR data. Based on these, vibrational spectroscopy have also been applied to study the solution chemistry of **1** in other solvents like 1.0 M HCl, acetone, methanol, ethanol, isopropanol, tetrahydrofuran, nitromethane, and benzyl alcohol (Figures S7–S11). It was found that under ambient conditions, **1** is stable in these solvents, too.

Compound **1** was synthesized by one-pot reaction of TiCl_4 (1.0 M), H_2SO_4 (0.33 M), and TBAC (1.0 M) in water under ambient conditions. The yield is ca. 69% (based on Ti). Increasing the concentration of H_2SO_4 to 1.0 M yielded **2**, while using 2.0 M $(\text{TBA})_2\text{SO}_4$ gave **3** (see SI for full formula of **2** and **3**), both having the same $\text{Ti}_{18}\text{O}_{27}$ cluster cores (Figure 3). **2**

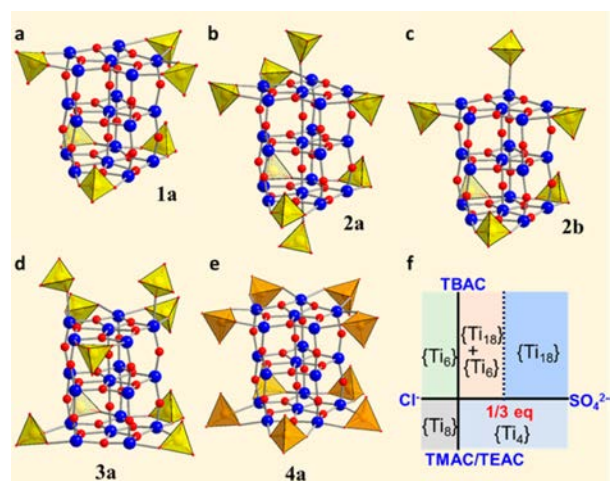


Figure 3. (a–e) Arrangements of the SO_4 groups (the yellow tetrahedrons) in **1a**–**3a** and the SeO_4 groups (the orange tetrahedrons) in **4a**. For clarity, the aqua ligands are not shown. (f) A model illustrating the regions of compound crystallization from the $\text{TiCl}_4/\text{SO}_4^{2-}$ system with R_4N^+ ($\text{R} = \text{CH}_3$, C_2H_5 or $n\text{-C}_4\text{H}_9$). In detail, a 1:1 mixture of TiCl_4 and TBAC gives the $[\text{Ti}_6\text{O}_8(\text{OH}_2)_{20}]^{8+}$ ($\{\text{Ti}_6\}$);^{8a} a 1:1 mixture of TiCl_4 and tetraethylammonium (TEA) or tetramethylammonium (TMA) chloride gives the $[\text{Ti}_8\text{O}_{12}(\text{OH}_2)_{24}]^{8+}$ ($\{\text{Ti}_8\}$);^{8b} TiCl_4 and H_2SO_4 (regardless of ratio) in the presence of TEAC/TMAC yields $[\text{Ti}_4\text{O}_4(\text{OH}_2)_8(\text{SO}_4)_4]$ ($\{\text{Ti}_4\}$);^{8a} reaction of TiCl_4 with less than 1/3 equiv of SO_4^{2-} in the presence of TBAC gives a mixture of $\{\text{Ti}_{18}\text{O}_{27}\}$ and $\{\text{Ti}_6\}$. $\{\text{Ti}_4\}$, $\{\text{Ti}_6\}$, and $\{\text{Ti}_8\}$ decompose upon dissolution in water.

contains two cluster structures, $[\text{Ti}_{18}\text{O}_{27}(\text{OH}_2)_{28}(\text{SO}_4)_8]^{2+}$ (**2a**) and $[\text{Ti}_{18}\text{O}_{27}(\text{OH}_2)_{31}(\text{SO}_4)_6]^{6+}$ (**2b**). In **2a** there are six SO_4^{2-} ligands in the same locations as in **1a** and another two monodentate SO_4^{2-} binding to the two seven-coordinated Ti-atoms, respectively, while in **2b** there are five SO_4^{2-} ligands at the side faces (of the $\text{Ti}_{18}\text{O}_{27}$ framework) and one more at the top face as monodentate ligand. **3** contains a cluster $[\text{Ti}_{18}\text{O}_{27}(\text{OH}_2)_{26}(\text{SO}_4)_9]$ (**3a**) with nine SO_4^{2-} ligands, of which seven are bidentate bridged to the side faces and the other two are monodentate bonded to the six-coordinated Ti-atoms at the top face. Both **2** and **3** are soluble and stable in 1.0 M HCl, MeCN, and acetone (Figures S12 and S13). When H_2SeO_4 was used instead of H_2SO_4 , compound **4** (see SI for full formula) containing $[\text{Ti}_{18}\text{O}_{27}(\text{OH}_2)_{24}(\text{SeO}_4)_9]$ (**4a**) of nine SeO_4^{2-}

ligands was exclusively obtained regardless of SeO_4^{2-} concentration in which the nine bridging bidentate SeO_4^{2-} ligands are located at the top and the bottom circumferences of the $\{\text{Ti}_{18}\text{O}_{27}\}$ pentagonal prism. **4** is of low solubility in acidic water but is very soluble and stable in alcohols (Figure S14).

Figure 3f demonstrates that the clusters featuring the $\text{Ti}_{18}\text{O}_{27}$ core are formed under a relatively wide range of conditions in the $\text{TiCl}_4/\text{XO}_4^{2-}$ aqueous system ($\text{X} = \text{S}$ or Se), which is one of the most important systems for titanate hydrosol/nanoparticle synthesis. It appears both SO_4^{2-} and the alkyl chain length of the R_4N^+ ions are dominating the formation and crystallization of the polycationic titanium-oxo clusters from water. We consider that near the surfaces of the polycationic $\{\text{Ti}_{18}\text{O}_{27}\}$ clusters, both the SO_4^{2-} ligands and the Cl^- counterions (Cl^- is hydrogen-bonded to the aqua ligands^{8b}) can associate with the coexisting TBA^+ cations via electrostatic interaction, which is the key in synthesis of the $\{\text{Ti}_{18}\text{O}_{27}\}$ clusters.

The present $\{\text{Ti}_{18}\text{O}_{27}\}$ cluster compounds can be used to functionalize nanomaterial surfaces (e.g., GO) and electrode surfaces.¹⁶ Adsorption of **1** on the GO surface was performed by adding GO sample to an MeCN (or 1.0 M HCl) solution of **1**, and ultrafiltration gave a wet solid residue, which was dried under vacuum. FTIR of the sample was measured (Figure 4A), and the

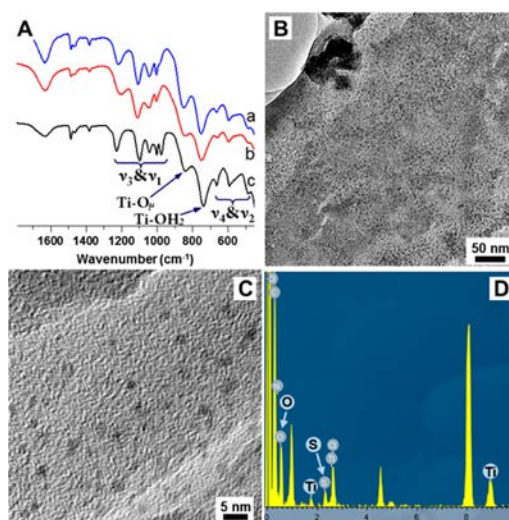


Figure 4. (A) FTIR spectra of **1**/GO prepared using a 1/1.0 M HCl solution (curve a) or a 1/MeCN solution (curve b), and that of the authentic solid sample (curve c). (B,C) TEM images of **1**/GO. (D) EDS analysis of a region in panel B demonstrating the existence of Ti, O, and S elements. In panel A, the Ti-O_μ and Ti-OH_2 stretching modes are hardly changed, while those of SO_4 ($\nu_1 - \nu_4$) are slightly changed due to adsorption on the GO surface.

data indicates the structural integrity of the $\text{Ti}_{18}\text{O}_{27}$ framework. This observation is consistent with the solution stability of **1**, as well as the thermogravimetric analysis results (Figure S15), which suggests that terminal aqua ligands are hardly lost at <200 °C. Due to the ultrathin nature of the GO sheet (1.1 nm), the **1**/GO nanocomposite is suitable for characterization of **1** with transmission electron microscopy (TEM). The TEM images show that on the surface of GO, there are many electron dense objects of ca. 1.5 nm (Figure 4B,C) consistent with the dimension of **1a**. Energy dispersive spectroscopy (EDS) was used to confirm these objects are molecules of **1** (Figure 4D).

The UV–vis absorption spectra of MeCN solutions of **1** (Figure S16) show that the absorption onset occurs at

approximately 420 nm. The extinction coefficient is $270 \text{ M}^{-1} \text{ cm}^{-1}$ at 380 nm and is $1.03 \times 10^5 \text{ M}^{-1} \text{ cm}^{-1}$ at 242 nm. Hence, we examined the photocatalytic activity of **1** under UV irradiation. First, **1** was adsorbed on a TiO_2/FTO photoanode surface following the analogous protocol as that for preparing the **1**/GO nanocomposite (see SI for experimental details). The obtained photoanode, **1**/ TiO_2/FTO , was then used for the short-circuit photocurrent test, and a dramatic enhancement of the photocurrent was observed (by up to 200% comparing to the unmodified TiO_2/FTO photoanode; Figure S18). This might be attributed to the enhancement of surface roughness and/or of the photoabsorption properties of the photoanode by **1a**. **1** was also found to be an active homogeneous photocatalyst to activate molecular O_2 for selective oxidation of benzyl alcohol to benzaldehyde.¹⁷ Conversion reached ca. 41% after 140 min, corresponding to a turnover number (TON; defined as $n(\text{converted benzyl alcohol})/n(\mathbf{1})$) of 67, giving benzaldehyde as a major kinetic product (yield = 40%). It is worth noting that during the above photocatalytic reactions, no precipitate or colloid was formed, and the vibrational spectroscopic analysis confirmed the stability of **1** (Figures S19–S21).

In summary, a new family of $\{\text{Ti}_{18}\text{O}_{27}\}$ titanium-oxo clusters, which possess a unique pentagonal-prismatic framework, are reported herein. Their ESI-MS, ^{17}O NMR, and vibrational spectroscopy have been elucidated. This type of molecular titanium oxide exhibits good photoactivities and photostabilities under oxidative and aqueous conditions. The above features will make them as promising titanium oxide molecular materials for many applications.

■ ASSOCIATED CONTENT

● Supporting Information

The Supporting Information is available free of charge on the ACS Publications website at DOI: 10.1021/jacs.6b06290.

Experimental details, structural views, characterization, catalysis, and more analysis (PDF)
X-ray crystallographic data (CIF)

■ AUTHOR INFORMATION

Corresponding Author

*yifeng@sdu.edu.cn

Notes

The authors declare no competing financial interest.

■ ACKNOWLEDGMENTS

Y.W. thanks the NSFC (21473104, 21401117), the NSF of Shandong Province (ZR2014BQ003), and the China Postdoctoral Science Foundation (2015MS72042). C.-H.T. thanks Shandong University for a startup fund (104.205.2.5). L.C. thanks the EPSRC (Grant No EP/J00135X/1).

■ REFERENCES

- (1) (a) Wang, S.; Yang, G. *Chem. Rev.* **2015**, *115*, 4893–4962. (b) Cronin, L.; Müller, A. *Chem. Soc. Rev.* **2012**, *41*, 7333–7334. (c) Weinstock, I. A.; Müller, A. *Isr. J. Chem.* **2011**, *51*, 176–178. (d) Hill, C. L. *Chem. Rev.* **1998**, *98*, 1–2.
- (2) (a) Lv, Y.; Cheng, J.; Steiner, A.; Gan, L.; Wright, D. S. *Angew. Chem., Int. Ed.* **2014**, *53*, 1934–1938. (b) Snoeberger, R. C.; Young, K. J.; Tang, J.; Allen, L. J.; Crabtree, R. H.; Brudvig, G. W.; Coppens, P.; Batista, V. S.; Benedict, J. B. *J. Am. Chem. Soc.* **2012**, *134*, 8911–8917. (c) Sokolow, J. D.; Trzop, E.; Chen, Y.; Tang, J.; Allen, L. J.; Crabtree, R. H.; Benedict, J. B.; Coppens, P. *J. Am. Chem. Soc.* **2012**, *134*, 11695–11700. (d) Benedict, J. B.; Freindorf, R.; Trzop, E.; Cogswell, J.;

Coppens, P. *J. Am. Chem. Soc.* **2010**, *132*, 13669–13671. (e) Benedict, J. B.; Coppens, P. *J. Am. Chem. Soc.* **2010**, *132*, 2938–2944.

(3) (a) Chen, Y.; Jarzemska, K. N.; Trzop, E.; Zhang, L.; Coppens, P. *Chem. - Eur. J.* **2015**, *21*, 11538–11544. (b) Coppens, P.; Chen, Y.; Trzop, E. *Chem. Rev.* **2014**, *114*, 9645–9661. (c) Rozes, L.; Sanchez, C. *Chem. Soc. Rev.* **2011**, *40*, 1006–1030.

(4) (a) Schneider, J.; Matsuoka, M.; Takeuchi, M.; Zhang, J.; Horiuchi, Y.; Anpo, M.; Bahnemann, D. W. *Chem. Rev.* **2014**, *114*, 9919–9986. (b) Chen, X.; Shen, S.; Guo, L.; Mao, S. S. *Chem. Rev.* **2010**, *110*, 6503–6570. (c) Chen, X.; Mao, S. S. *Chem. Rev.* **2007**, *107*, 2891–2959. (d) Hoffmann, M. R.; Martin, S. T.; Choi, W.; Bahnemann, D. W. *Chem. Rev.* **1995**, *95*, 69–96.

(5) For the early reports on titanium-oxo clusters, see: (a) Bradley, D. C.; Gaze, R.; Wardlaw, W. J. *Chem. Soc.* **1955**, 3977–3982. (b) Ibers, J. A. *Nature* **1963**, *197*, 686–687. (c) Martin, R. L.; Winter, G. *Nature* **1963**, *197*, 687.

(6) Matthews, P. D.; King, T. C.; Wright, D. S. *Chem. Commun.* **2014**, *50*, 12815–12823.

(7) For the discussion on nonclassical crystal growth theory, see: (a) Ruther, R. E.; Baker, B. M.; Son, J.; Casey, W. H.; Nyman, M. *Inorg. Chem.* **2014**, *53*, 4234–4242. (b) Niederberger, M.; Cölfen, H. *Phys. Chem. Chem. Phys.* **2006**, *8*, 3271–3287. (c) Navrotsky, A. *Proc. Natl. Acad. Sci. U. S. A.* **2004**, *101*, 12096–12101. (d) Penn, R. L.; Banfield, J. F. *Geochim. Cosmochim. Acta* **1999**, *63*, 1549–1557. (e) Penn, R. L.; Banfield, J. F. *Am. Mineral.* **1998**, *83*, 1077–1082 and the references therein.

(8) (a) Zhang, G.; Hou, J.; Tung, C.-H.; Wang, Y. *Inorg. Chem.* **2016**, *55*, 3212–3214. (b) Zhang, G.; Hou, J.; Li, M.; Tung, C.; Wang, Y. *Inorg. Chem.* **2016**, *55*, 4704–4709. (c) Reichmann, M. G.; Hollander, F. J.; Bell, A. T. *Acta Crystallogr., Sect. C: Cryst. Struct. Commun.* **1987**, *C43*, 1681–1683.

(9) Kong, X.; Long, L.; Zheng, Z.; Huang, R.; Zheng, L. *Acc. Chem. Res.* **2010**, *43*, 201–209.

(10) (a) Zhan, C.; Winter, R. S.; Zheng, Q.; Yan, J.; Cameron, J. M.; Long, D.; Cronin, L. *Angew. Chem., Int. Ed.* **2015**, *54*, 14308–14312. (b) Müller, A.; Gouzerh, P. *Chem. Soc. Rev.* **2012**, *41*, 7431–7463. (c) Long, D.; Tsunashima, R.; Cronin, L. *Angew. Chem., Int. Ed.* **2010**, *49*, 1736–1758.

(11) (a) Yan, J.; Gao, J.; Long, D.; Miras, H. N.; Cronin, L. *J. Am. Chem. Soc.* **2010**, *132*, 11410–11411. (b) Todea, A. M.; Merca, A.; Bögge, H.; Glaser, T.; Engelhardt, L.; Prozorov, R.; Luban, M.; Müller, A. *Chem. Commun.* **2009**, 3351–3353.

(12) Tsunashima, R.; Long, D.; Miras, H. N.; Gabb, D.; Pradeep, C. P.; Cronin, L. *Angew. Chem., Int. Ed.* **2010**, *49*, 113–116.

(13) (a) Gao, M.; Wang, F.; Gu, Z.; Zhang, D.; Zhang, L.; Zhang, J. *J. Am. Chem. Soc.* **2016**, *138*, 2556–2559. (b) Chen, Y.; Trzop, E.; Makal, A.; Chen, Y.; Coppens, P. *Dalton Trans.* **2014**, *43*, 3839–3841. (c) Chen, Y.; Trzop, E.; Makal, A.; Sokolow, J. D.; Coppens, P. *Inorg. Chem.* **2013**, *52*, 4750–4752. (d) Lv, Y.; Willkomm, J.; Leskes, M.; Steiner, A.; King, T. C.; Gan, L.; Reiser, E.; Wood, P. T.; Wright, D. S. *Chem. - Eur. J.* **2012**, *18*, 11867–11870.

(14) (a) Liu, Z.; Lei, J.; Frascioni, M.; Li, X.; Cao, D.; Zhu, Z.; Schneebeli, S. T.; Schatz, G. C.; Stoddart, J. F. *Angew. Chem., Int. Ed.* **2014**, *53*, 9193–9197. (b) Fornasieri, G.; Rozes, L.; Le Calvé, S.; Alonso, B.; Massiot, D.; Rager, M. N.; Evain, M.; Boubekeur, K.; Sanchez, C. *J. Am. Chem. Soc.* **2005**, *127*, 4869–4878. (c) Day, V. W.; Eberspacher, T. A.; Klemperer, W. G.; Park, C. W.; Rosenberg, F. S. *J. Am. Chem. Soc.* **1991**, *113*, 8190–8192.

(15) Steunou, N.; Ribot, F.; Boubekeur, K.; Maquet, J.; Sanchez, C. *New J. Chem.* **1999**, *23*, 1079–1086.

(16) (a) Georgakilas, V.; Tiwari, J. N.; Kemp, K. C.; Perman, J. A.; Bourlinos, A. B.; Kim, K. S.; Zboril, R. *Chem. Rev.* **2016**, *116*, 5464–5519. (b) Chen, D.; Feng, H.; Li, J. *Chem. Rev.* **2012**, *112*, 6027–6053. (c) Wang, Y.; Weinstock, I. A. *Chem. Soc. Rev.* **2012**, *41*, 7479–7496.

(17) (a) Lang, X.; Ma, W.; Chen, C.; Ji, H.; Zhao, J. *Acc. Chem. Res.* **2014**, *47*, 355–363. (b) Zhang, M.; Wang, Q.; Chen, C.; Zang, L.; Ma, W.; Zhao, J. *Angew. Chem., Int. Ed.* **2009**, *48*, 6081–6084.